Synthesis of Eight-bar Linkages by Constraining a 6R Loop

K. H. Sonawale[a,*], J. M. McCarthy[a]

[a]*Robotics and Automation Laboratory,Mechanical and Aerospace Engineering, University of California, Irvine, California 92697, USA*

Abstract

This paper presents a design system for planar eight-bar linkages that begins with a user specified 6R planar loop and five required configurations, and computes two RR constraints that yield an eight-bar linkage. There are 32 ways that these constraints can be added to the 6R loop to yield as many as 340 different linkages, which include eight of the 16 eight-bar linkage topologies. An analysis routine based on the Dixon determinant is used to verify the performance of each design candidate. Random variation of task configurations within user specified tolerance zones is used to increase the number of candidate designs. The result is an effective system for the design of eight-bar linkages, which is demonstrated by designing linkages that guide movement though a symmetric and offset set of parallel task positions along a straight line.

1. Introduction

This paper presents a design system for eight-bar linkages that adds two RR dyads to a user-specified 6R planar loop shown in Figure 1. The approach specifies five configurations and then uses five-position synthesis of two RR dyads to constrain the relative movement of links in the 6R loop to obtain an eight-bar linkage.

The design system generates all of the candidate linkages available from the 32 ways the 6R loop can be constrained, and then evaluates their per-

*Corresponding author

Email addresses: ksonawal@uci.edu (K. H. Sonawale), jmmccart@uci.edu (J. M. McCarthy)

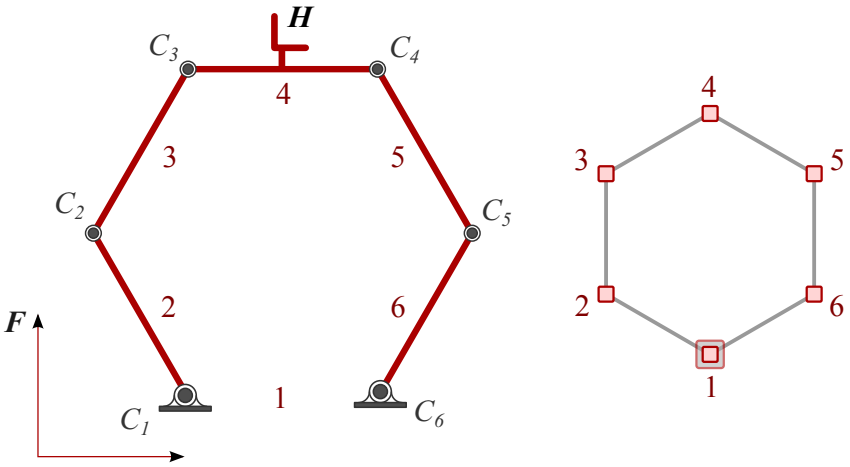

Figure 1: A 6R loop with hinged joints $C_1, \ldots, C_6$ and links $\{1, \ldots, 6\}$, together with its linkage graph. Notice that the ground is link 1 and the end-effector is link 4.

formance to ensure successful designs. The number of design candidates is increased by varying the task requirements within user specified tolerance zones. This system is demonstrated by finding successful eight-bar linkage designs for a set of parallel task positioned on a straight line.

2. Literature Review

A design theory for linkages with six, eight and 10-bars was presented by Kempe (1877), who provided geometric techniques for the design of 8-bar linkages that trace an exact straight line. Mueller (1954) introduced a graphical approach for the synthesis of an eight-bar linkage. Also see the work of Hain (1967) and Hamid and Soni (1973). Chen and Angeles (2008) developed a method to synthesize an eight-bar linkage obtained by coupling two four-bar linkages that can reach 11 specified task positions.

The use of two RR dyad to transform a 6R loop into an eight-bar linkage was introduced by Soh and McCarthy (2007). Central to this process is the calculation of an RR dyad that connects two relatively moving bodies introduced by Burmester (1888), also Sandor et al. (1984). For a discussion of Burmester's work see Koetsier (1989).

The designer specifies five task configurations for the 6R loop, and the design system calculates the inverse kinematics of the system to determine

the position and orientation every link in the system, Murray et al. (1994). The synthesis routine uses a graph theory based procedure to identify the RR dyads that yield eight-bar linkages. This provides an automated way to formulate the design equations for the 32 different cases yielding eight of the sixteen eight-bar linkage topologies, McCarthy and Soh (2010).

The design system analyzes each candidate design in order to verify performance. This is done using the analysis algorithm developed by Parrish et al. (2014), which uses the adjacency matrix of a linkage graph to characterize the design, Tsai (2000).

This paper is an extension of research on eight-bar linkage design system presented in Sonawale and McCarthy (2014); Sonawale (2015). The initial results in this area focused on adding three RR dyads to a 4R serial chain can be found here, Sonawale and McCarthy (2015). Examples show this design system yields a large number of successful designs even for a parallel set of task positions distributed on a straight line.

3. Synthesis of an RR Constraint

The usual formulation of Burmester's synthesis equations assumes that the RR constraint connects a moving body M to a fixed body F. This can be generalized for the purposes of this design system, by assuming five positions of the first moving body represented by frames M_j and five positions of the second moving body represented by frames F_j, $j = 1, \ldots 5$, are known. Let the 3×3 homogeneous transformations $[R_j]$ and $[S_j]$ define the position and orientation of M_j and F_j, $j = 1, \ldots 5$, respectively, in the ground frame, given by,

$$[R_j] = \begin{bmatrix} \cos\gamma_j & -\sin\gamma_j & a_j \\ \sin\gamma_j & \cos\gamma_j & b_j \\ 0 & 0 & 1 \end{bmatrix}, \; [S_j] = \begin{bmatrix} \cos\sigma_j & -\sin\sigma_j & c_j \\ \sin\sigma_j & \cos\sigma_j & d_j \\ 0 & 0 & 1 \end{bmatrix}, \quad j = 1, \ldots, 5. \tag{1}$$

Let $\mathbf{w} = (w_x, w_y, 1)$ be the homogeneous coordinates of point fixed in the frame M and, similarly, let $\mathbf{g} = (g_x, g_y, 1)$ be fixed in F, so

$$\mathbf{W}^j = [R_j]\mathbf{w}, \quad \mathbf{G}^j = [S_j]\mathbf{g}, \quad j = 1, \ldots, 5. \tag{2}$$

The constraint equations for an RR crank that connect the frames M_j and F_j, $j = 1, \ldots 5$, are given by,

$$(\mathbf{W}^j - \mathbf{G}^j) \cdot (\mathbf{W}^j - \mathbf{G}^j) = R^2, \quad j = 1, \ldots, 5, \tag{3}$$

where the dot denotes the usual vector dot product, and R is a constant that defines the length of the RR crank. These five equations can be solved for the coordinates of $\mathbf{w}$ and $\mathbf{g}$ and the length R.

It is convenient to reformat the equations in (2) so that the coordinates of the RR crank pivots are defined in the ground frame G as $\mathbf{W}^1 = (x, y, 1)$ and $\mathbf{G}^1 = (u, v, 1)$. This is done by introducing the relative transformations,

$$[R_{1j}] = [R_j][R_1]^{-1} \quad [S_{1j}] = [S_j][S_1]^{-1}, \quad j = 1, \ldots, 5, \tag{4}$$

so that

$$\mathbf{W}^j = [R_{1j}]\mathbf{W}^1 \quad \mathbf{G}^j = [S_{1j}]\mathbf{G}^1, \quad j = 1, \ldots, 5. \tag{5}$$

The constraint equations for the RR crank now take the form,

$$([R_{1j}]\mathbf{W}^1 - [S_{1j}]\mathbf{G}^1) \cdot ([R_{1j}]\mathbf{W}^1 - [S_{1j}]\mathbf{G}^1) = R^2 \\ j = 1, \ldots, 5. \tag{6}$$

Subtract the first of the equations (6) from the remaining to eliminate R^2 and obtain the four bilinear synthesis equations in four unknowns, $\mathbf{r} = (u, v, x, y)$ as,

$$([R_{1j}]\mathbf{W}^1 - [S_{1j}]\mathbf{G}^1) \cdot ([R_{1j}]\mathbf{W}^1 - [S_{1j}]\mathbf{G}^1) - (\mathbf{W}^1 - \mathbf{G}^1) \cdot (\mathbf{W}^1 - \mathbf{G}^1) = 0, \\ j = 2, \ldots, 5. \tag{7}$$

The solution of these synthesis equations yields as many as four sets of design parameters, $\mathbf{r} = (u_i, v_i, x_i, y_i)$, $i = 1, 2, 3, 4$, defining the RR cranks $\mathbf{W}^1\mathbf{G}^1$. See Burmester (1888), Sandor et al. (1984) and McCarthy and Soh (2010).

4. Attachment of RR Dyads to a 6R Loop

In order to manage the attachment of two RR dyads to a 6R planar loop, we introduce its linkage graph, see Tsai (2000). Let the graph, $G =< V, E >$, be defined by the list of links V and the list of joints E, which represent the two links they connect. Our convention for numbering the links of a 6R loop is shown in Figure 1.

This yields a linkage graph for the 6R loop defined by,

$$\begin{aligned} G &=< V, E > \\ &=< \{1, 2, 3, 4, 5, 6\}, \{\{1, 2\}, \{2, 3\}, \{3, 4\}, \{4, 5\}, \{5, 6\}, \{1, 6\}\} > . \end{aligned} \tag{8}$$

The eight-bar linkages obtained by adding two RR dyads to a 6R loop can be viewed as defined by the linkage graphs $L_{(ij)(kl)}$ obtained from G by adding two subgraphs,

$$\begin{aligned} A_{ij} &= < \{i, j, 7\}\,, \{\{i, 7\}, \{j, 7\}\} >, \\ B_{kl} &= < \{k, l, 8\}\,, \{\{k, 8\}, \{l, 8\}\} > . \end{aligned} \tag{9}$$

The vertices (i, j) and (k, l) are to be enumerated to determine all possible eight-bar linkages given by,

$$L_{(ij)(kl)} = G \cup \{\{7, 8\}\,, \{\{i, 7\}, \{j, 7\}, \{k, 8\}, \{l, 8\}\}\}. \tag{10}$$

In order to enumerate the linkage graphs, $L_{(ij)(kl)}$, we introduce the vertex list V_6 of the 6R closed chain and the vertex list V_7 of the linkage after A_{ij} is attached. Enumeration of pairs of vertices in the lists V_6 and V_7 that are available for the attachment of the RR dyads yields the lists P_A and P_B,

$$\begin{aligned} P_A =& \{(i, j) : i, j \in V_6, i \neq j\},\ |P_A| = \binom{6}{2} = 15, \\ P_B =& \{(k, l) : k, l \in V_7, k \neq l\},\ |P_B| = \binom{7}{2} = 21. \end{aligned} \tag{11}$$

This shows that the maximum number of linkage graphs, $L_{(ij)(kl)}$ obtained by combination of these lists is given by,

$$|L_{(ij)(kl)}| = |P_A||P_B| = 315. \tag{12}$$

However, these 315 linkage graphs are reduced by constraints imposed to eliminate duplicate graphs, to remove links that combine to form a structure, and to add preferred design features to the eight-bar linkage.

4.1. Ordering

The possibility that two different linkage graphs describe the same eight-bar linkage can be eliminated by introducing an ordering to the labeling of the attached RR dyads. Specifically, introduce the convention,

$$i < j, \quad k < l. \tag{13}$$

Now, order the linkage graphs $L_{(ij)(kl)}$, such that the pairs $(ij)(kl)$ are listed in order of the first entries i and k and then in order of the second entries j

and l. This means the two dyads connecting links $\{2, 6\}$ and $\{3, 5\}$ are listed as (26)(35) while the dyads connecting links $\{2, 6\}$ and $\{2, 3\}$, are listed as (23)(26).

This ordering eliminates 105 duplicate graphs reducing the number of linkage graphs to 210.

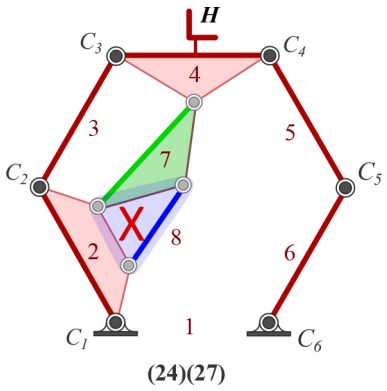

Figure 2: RR dyads connecting the links $\{2, 7, 8\}$ yields three joints $\{\{2, 7\}, \{2, 8\}, \{7, 8\}\}$ that form a structure.

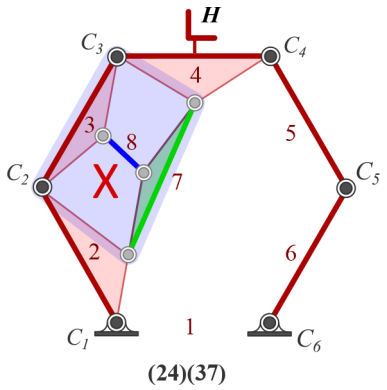

Figure 3: The sequence of links $\{2, 3, 4, 7\}$ form a quadrilateral. A dyad connecting vertices $\{2, 4\}$ or $\{3, 7\}$ forms a structure.

4.2. Structure Subgraphs

There are two cases in which the addition of two RR dyads creates a substructure, which collapses several links into one. The two cases are at-

tachments that:

1. Form a triangle: If three links $\{r, s, t\}$ are connected by three joints $\{\{r, s\}, \{s, t\}, \{t, r\}\}$, the result is a pin-jointed triangle which forms a structure with no relative movement. An example is the sequence of edges $\{\{2, 7\}, \{2, 8\}, \{7, 8\}\}$ shown in Figure 2.
2. Connect opposite sides of a quadrilateral: If four vertices $\{r, s, t, w\}$ form a quadrilateral, then the addition of a dyad connecting either $\{r, t\}$ or $\{s, w\}$ will forms a structure with no relative movement. Figure 3 shows the case where links $\{2, 3, 4, 7\}$ forms a structure with the addition of the dyad connecting $\{3, 7\}$.

Eliminating the linkage graphs that have these substructures reduces the number of eight-bar linkage graphs to 69.

4.3. Design features

This last condition is artificial in the sense that it imposed to achieve designs that have a particular feature. Our experience shows that an important concern of linkage designers is the location of attachment points to the ground frame. For this reason, we restrict the eight-bar linkage graphs to include only the two connections to the ground frame that were specified as part of the 6R loop. This removes 37 linkage graphs that include a third base pivot. The result is 32 eight-bar linkage graphs.

5. The Design Requirements

The eight-bar linkage design system requires specification of the five task positions for the end-effector and the dimensions of the 6R loop in the first position, see Figure 4. Specifically, the user defines the following requirements,

1. the five transformations, $[D_j], j = 1, \ldots, 5$, that define the movement of the end-effector frame,

$$[D_j] = \begin{bmatrix} \cos\phi_j & -\sin\phi_j & d_{1x,j} \\ \sin\phi_j & \cos\phi_j & d_{1y,j} \\ 0 & 0 & 1 \end{bmatrix}, \; j = 1, \ldots, 5; \tag{14}$$

2. the coordinates of the two base pivots, $C_1 : \mathbf{g_1} = (g_{1x}, g_{1y}, 1)$, and $C_6 : \mathbf{g_2} = (g_{2x}, g_{2y}, 1)$;

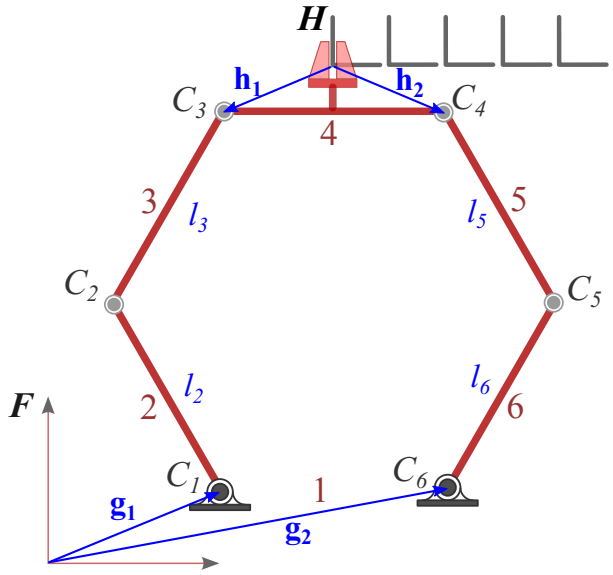

Figure 4: Five required task positions, and the configuration of the 6R loop in the first position.

3. the coordinates of the two moving pivots attached to the end-effector, measured in the end-effector frame, C_3 : $\mathbf{h_1} = (h_{1x}, h_{1y}, 1)$ and C_4 : $\mathbf{h_2} = (h_{2x}, h_{2y}, 1)$;
4. the dimensions, $l_2 = |C_1C_2|$, $l_3 = |C_2C_3|$, $l_5 = |C_4C_5|$ and $l_6 = |C_5C_6|$; and,
5. whether the elbow pivots C_2 and C_5 are configured in the positive or negative configurations.

This data is used to determine the position and orientation of each link of the 6R loop in each of the task positions. The relative positions of links in the 6R loop are then used to synthesis the RR dyads using equation (7).

5.1. Inverse kinematics of the 6R loop

The position and orientation of the each of the links of the 6R loop can be determined by considering the inverse kinematics of the two 3R chains, $\{C_1, C_2, C_3\}$ and $\{C_6, C_5, C_4\}$, that form the 6R loop, see Figure 4.

Using the Denavit Hartenberg convention, the kinematics equations for

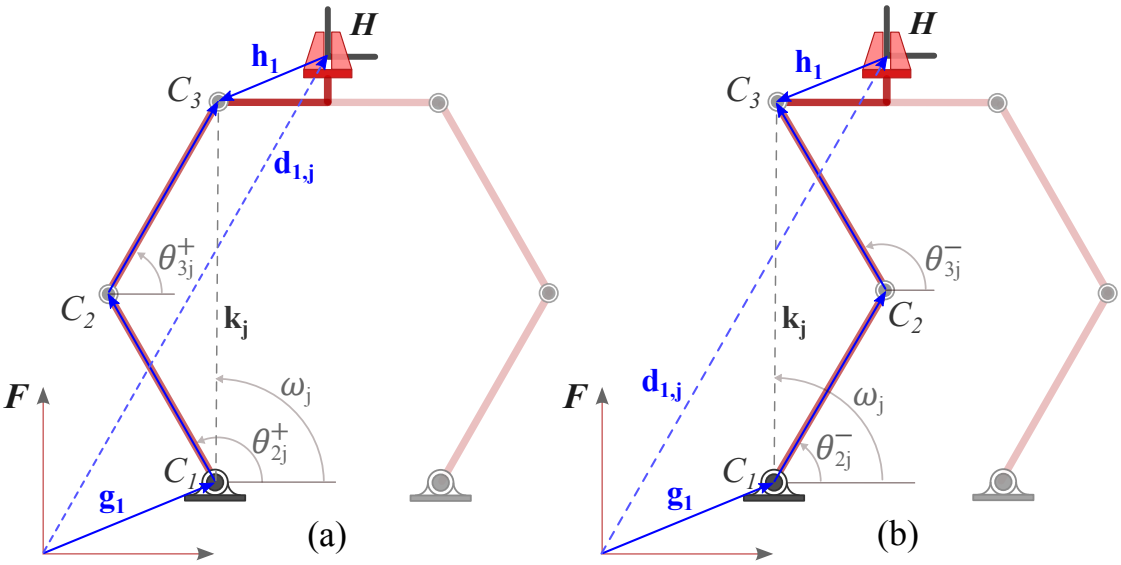

Figure 5: (a) is the positive configuration for elbow C_2, and (b) is the negative configuration for elbow C_2 for the left 3R chain $\{C_1, C_2, C_3\}$.

the 3R chain $\{C_1, C_2, C_3\}$ are given as,

$$[D_j] = [T(\mathbf{g}_1)][Z(\theta_{2,j})][X(l_2)][Z(\theta_{3,j} - \theta_{2,j})][X(l_3)][Z(\phi_j - \theta_{3,j})][T(-\mathbf{h}_1)], \quad j = 1, \ldots, 5; \tag{15}$$

where the homogenous transformation matrices $[T(\mathbf{g})], [Z(\theta)]$ and $[X(l)]$ and are given as,

$$[T(\mathbf{g})] = \begin{bmatrix} 1 & 0 & g_x \\ 0 & 1 & g_y \\ 0 & 0 & 1 \end{bmatrix}, [Z(\theta)] = \begin{bmatrix} \cos\theta & -\sin\theta & 0 \\ \sin\theta & \cos\theta & 0 \\ 0 & 0 & 1 \end{bmatrix}, [X(l)] = \begin{bmatrix} 1 & 0 & l \\ 0 & 1 & 0 \\ 0 & 0 & 1 \end{bmatrix}. \tag{16}$$

In order to determine the angles $\theta_{2,j}$ and $\theta_{3,j}$, rearrange the kinematics equations into the form,

$$[K_j] = [Z(\theta_{2,j})][X(l_2)][Z(\theta_{3,j} - \theta_{2,j})][X(l_3)][Z(-\theta_{3,j})], \quad j = 1, \ldots, 5; \tag{17}$$

where $[K_j]$ is the matrix of known constants,

$$[K_j] = [T(\mathbf{g}_1)]^{-1}[D_j][T(-\mathbf{h}_1)]^{-1}[Z(-\phi_j)]. \tag{18}$$

Expand equation 18 to obtain from the third column of $[K_j]$, the vector $\mathbf{k}_j = (k_{x,j}, k_{y,j})$, given by

$$\begin{aligned} k_{x,j} &= d_{1x,j} + h_{1x}\cos\phi_j - h_{1y}\sin\phi_j \\ k_{y,j} &= d_{1y,j} + h_{1y}\cos\phi_j + h_{1x}\sin\phi_j \end{aligned} \tag{19}$$

Next, simplify the right hand side of equation 17 to obtain,

$$\begin{aligned} k_{x,j} &= l_2\cos\theta_{2,j} + l_3\cos\theta_{3,j} \\ k_{y,j} &= l_2\sin\theta_{2,j} + l_3\sin\theta_{3,j}, \quad j = 1,\ldots,5. \end{aligned} \tag{20}$$

Introduce the angle ω_j that defines the direction of the vector $\mathbf{k}_j$, which is given by

$$\omega_j = \arctan\left(\frac{k_{y,j}}{k_{x,j}}\right), \quad j = 1,\ldots,5. \tag{21}$$

This combined with the cosine law of the triangle formed by $C_1C_2C_3$ yields,

$$\theta_{2,j} = \omega_j \pm \arccos\left(\frac{l_2^2 + |\mathbf{k}_j|^2 - l_3^2}{2l_2|\mathbf{k}_j|}\right), \quad j = 1,\ldots,5. \tag{22}$$

The arccos function yields positive and negative values for $\theta_{2,j}$, which correspond to the positive and negative configurations of the elbow C_2 as shown in Figure 5(a) and (b) respectively.

The angle $\theta_{3,j}$ is now obtained from the equation (20), as

$$\theta_{3,j} = \arctan\left(\frac{k_{y,j} - l_2\sin\theta_{2,j}}{k_{x,j} - l_2\cos\theta_{2,j}}\right). \tag{23}$$

A similar analysis yields the angles angles $\theta_{4,j}$ and $\theta_{5,j}$, the result is that the position and orientation of each link in the 6R loop is defined in each task position.

5.2. Synthesis equations

This data allows the determination of the position and orientation of each of the links, $V_\mu, \mu = 1, \ldots, 6$, of the 6R loop, in each of five task configurations, $D_\nu, \nu = 1, \ldots, 5$. The result is the set of transformations,

$$[K_{\mu,\nu}] = \begin{bmatrix} \cos\theta_{\mu,\nu} & -\sin\theta_{\mu,\nu} & a_{\mu,\nu} \\ \sin\theta_{\mu,\nu} & \cos\theta_{\mu,\nu} & b_{\mu,\nu} \\ 0 & 0 & 1 \end{bmatrix}, \quad \mu = 1, \ldots, 6, \quad \nu = 1, \ldots, 5. \tag{24}$$

The synthesis equations for an RR dyads between the links V_i and V_k are obtained by substituting,

$$[R_\nu] = [K_{i,\nu}], \ [S_\nu] = [K_{k,\nu}], \quad \nu = 1, \ldots, 5, \tag{25}$$

into equation (7). Notice that for convenience the symbol ν replaces the symbol j in the synthesis equations. Once the first RR constraint is applied, it is available for attachment for the second RR constraint. Hence, following the application of first RR constraint, which forms the link 7, the list of transformations, $[K_{\mu,\nu}]$ from equation 24, is updated for this new link 7.

6. Calculating Candidate Designs

The design system solves the synthesis equations (7), to calculate the two RR constraints, for each of the of the 32 unique linkage graphs $L_{(ij)(kl)}$. The number of solutions must account for RR constraint solutions that satisfy the synthesis equations and are already part of the linkage.

This is done by distinguishing two cases, (i) sets of two RR constraints that include only the vertices, $\{1, 2, 3, 4, 5, 6\}$ of the original 6R closed chain, which we refer to as independent constraints, and (ii) sets of two RR constraints, that include one connection to a vertex in the set $\{7\}$, which we refer as dependent constraints.

Independent constraints:. A set of two RR constraints that connect to the vertices $i, j, k, l \in \{1, 2, 3, 4, 5, 6\}$ can be applied independent of each other. There are 17 unique ways of attaching the independent constraints as shown in Fig.12.

In order to count the number of design candidates obtained from the synthesis equations, consider the linkage graph example (24)(26) shown in Figure 6. Observe that for the attachment of the first RR constraint A_{24},

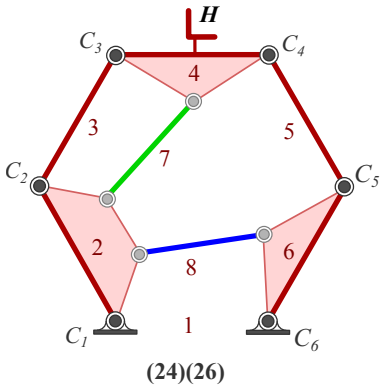

Figure 6: Eight-bar linkage graph (24)(26) can produce a maximum of 9 candidate linkage designs.

one solution C_2C_3 already exists, thus the synthesis equations yield at most three new RR constraints. This is true for the second RR constraint B_{26} as well. In this case, the various combinations of the RR solutions yields as many as $3 \times 3 = 9$ candidate designs.

A systematic count for all the 17 linkage graphs with independent constraints, yields as many as 178 eight-bar candidate linkage designs.

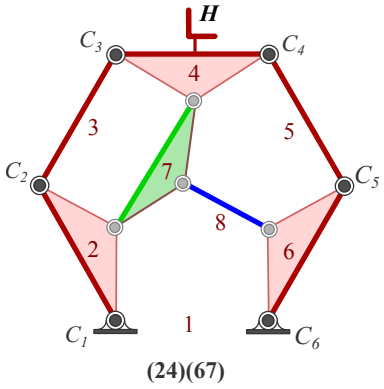

Figure 7: Eight-bar linkage graph (24)(67) can produce a maximum of 12 candidate linkage designs.

Dependent constraints:. A set of two RR constraints with $i, j, k \in \{1, 2, 3, 4, 5, 6\}$ and $l \in \{7\}$, will have the second RR constraint attached to

the first RR constraint. There are 15 unique ways of attaching the dependent constraints as shown in Fig.13.

In order to count the number of design candidates obtained from the synthesis equations, consider the linkage graph (24)(67) shown in Figure 7. Observe that for the attachment of the first RR constraint A_{24}, one solution C_2C_3 already exists, thus the synthesis equations yield at most three new RR constraints. For the application of second RR constraint B_{67}, all the four RR constraint solutions are available. In this case, the various combinations of the RR solutions yields as many as $3 \times 4 = 12$ candidate designs.

A systematic count for all the 15 linkage graphs with dependent constraints yields as many as 162 eight-bar linkage candidate designs.

Finally, this yields a total of 340 eight-bar designs for the 32 linkage graphs.

7. Performance Verification

The performance of a eight-bar linkage design is analyzed to determine the movement of the end-effector for each assembly. The end-effector must pass through the five task positions in a single assembly in order for the candidate linkage to be a successful design.

We use the automated system developed by Parrish et al. (2014) for the analysis of eight-bar linkages. This algorithm reads the location of the pivots of the eight-bar linkage in the first task position and the adjacency matrix of the linkage graph to formulate the three loop equations of the eight-bar linkage. These equations are solved analytically using the Dixon determinant approach in order to obtain all the assemblies of the linkage at each value of the input angle.

A sorting algorithm collects the result of the analysis routine into a maximum of 16 assemblies that define the values of the 10 joint angles for k iterations of the input angle θ_2. Note that θ_1 is the angle made by the ground link which remains constant. The results are the joint trajectories for each of the 16 assemblies,

$$\begin{aligned}
\Theta_1 &= \{\{\theta_{1,1}, \theta_{1,2}, \ldots, \theta_{1,10}\}_k\}, \quad k = 1, \ldots, n, \\
\Theta_2 &= \{\{\theta_{2,1}, \theta_{2,2}, \ldots, \theta_{2,10}\}_k\}, \quad k = 1, \ldots, n, \\
&\vdots \\
\Theta_{16} &= \{\{\theta_{16,1}, \theta_{16,2}, \ldots, \theta_{16,10}\}_k\}, \quad k = 1, \ldots, n.
\end{aligned} \tag{26}$$

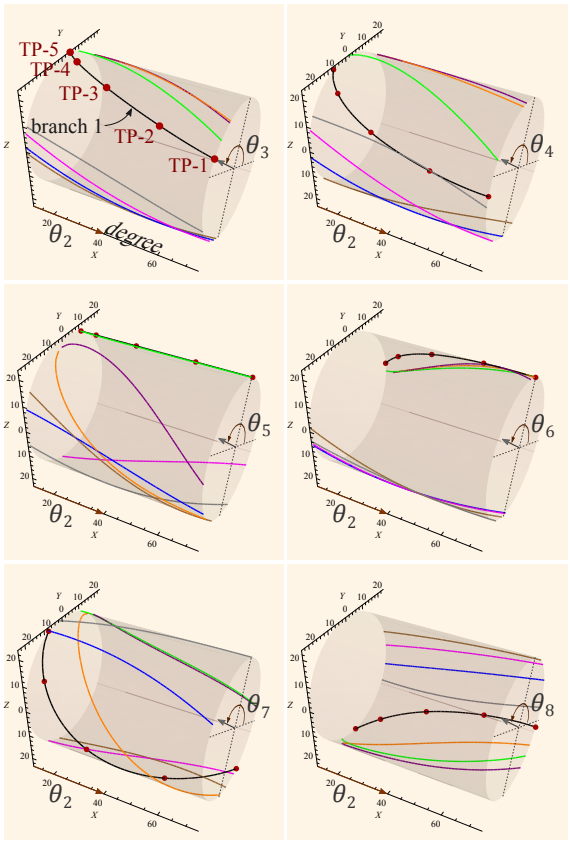

Figure 8: Configurations trajectories (branches) for an defect-free eight-bar linkage. All the five task position configurations lie on the same branch 1

For more details about sorting solutions into linkage assemblies to verify performance, see Plecnik and McCarthy (2013).

Figure 8 is an example where each assembly trajectory is represented by its joint angle $\theta_3, \ldots, \theta_{10}$ trajectories, for the given input joint angle θ_2. In order to meet the performance requirements, all the task positions must lie on one trajectory, or branch, for all the joint angles. In addition to this requirement the designer may also require the link lengths of the linkage to meet certain criteria to be of practical use.

8. Tolerance Zones

McCarthy and Choe (2010) showed that kinematic synthesis equations

regularly fail to yield designs that meet the performance requirements, because the task positions fall on separate branches. This challenge has been overcome by introducing small variations to the task within designer specified tolerance zones. The result is a reliable synthesis procedure that has been implemented in the MechGen series of design systems, Sonawale et al. (2013).

For the example of rectilinear motion linkage discussed later, we randomize the location of the ground pivots C_1 and C_6, instead of the task positions. The initial pass through the design algorithm, $k = 1$, uses the user defined task positions and 6R loop data $\{C_1, \ldots, C_6\}$. For each subsequent iteration $k = 2, \ldots, q$, where q are the number of iterations specified by the user, the ground pivots are randomized and successful eight-bar linkages are saved. The ground pivots $C_1 = \{C_{1x}, C_{1y}\}$ and $C_6 = \{C_{6x}, C_{6y}\}$ positions are modified by the addition of random variations in the tolerance zones $(\pm\Delta C_{1x}, \pm\Delta C_{1y})$ and $(\pm\Delta C_{6x}, \pm\Delta C_{6y})$ respectively, given by

$$\begin{aligned} C_{1k} =& \{C_{1x} + \text{Rand}(\pm\Delta C_{1x}), C_{1y} + Rand(\pm\Delta C_{1y})\} \\ C_{6k} =& \{C_{6x} + \text{Rand}(\pm\Delta C_{6x}), C_{6y} + Rand(\pm\Delta C_{6y})\}, \quad k = 2, \ldots, q. \end{aligned} \tag{27}$$

where Rand denotes the random selection of a value in the given range. This introduction of random variations to the ground pivots within user-defined tolerance zones increases the number of successful eight-bar linkage designs.

Table 1: Five parallel task positions along a straight line

Task	Orientation (θ) (degrees)	Location(x, y)
1	0°	(−50.0, 0.0)
2	0°	(−25.0, 0.0)
3	0°	(0.0, 0.0)
4	0°	(25.0, 0.0)
5	0°	(50.0, 0.0)

9. Design of Rectilinear Eight-bar Linkages

In order to demonstrate this design system, we present the synthesis of eight-bar linkages that trace a set of task positions on a straight line. Two

Table 2: 6R closed chain symmetric to the task positions.

Pivot	Location(x, y)
C_1	$(-50.00, -150.00)$
C_2	$(-142.11, -110.81)$
C_3	$(-100.00, -20.00)$
C_4	$(0.00, -20.00)$
C_5	$(91.98, -59.24)$
C_6	$(50.00, -150.00)$

Table 3: Number of successful eight-bar designs for symmetric task positions

Iterations	Linkage Candidates	Successful Designs	Computation Time
1	46	9	0.737 min
10	411	98	7.084 min
100	4583	1031	68.208 min

cases are shown (i) five task positions that are place symmetrically relative to the 6R loop, and (ii) five task positions that start at the center and extend to one side.

9.1. Symmetric task positions

The five task positions selected for this example extend over 100mm and are separated by 25mm, see Tab.1. The 6R loop was initially specified as hexagon with 100mm sides, however, this symmetry does not produce solutions. This was corrected by introducing a 0.1mm addition to the length of the links C_1C_2 and C_2C3, that is $|C_2C_3| = |C_2C_3| = 100.1$mm. The resulting joint coordinates of the 6R closed chain in the first task position is given in Table2.

In order to expand the number of potential designs, a random variation within $\pm$5mm was introduced for both the (x, y) coordinates of the ground pivots C_1 and C_6. The number of eight-bar designs for $1, 10$ and 100 iterations are shown in Table 3. The calculations were performed on an AMD Phenom II, 3.3 GHz, 6 core desktop computer.

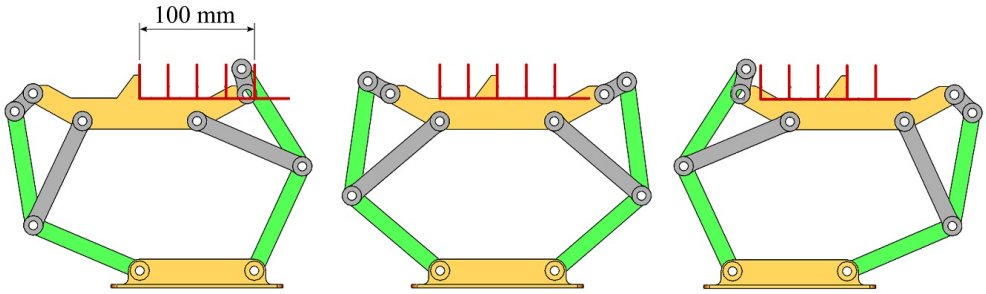

Figure 9: An eight-bar linkage design obtained for the symmetric set of task positions.

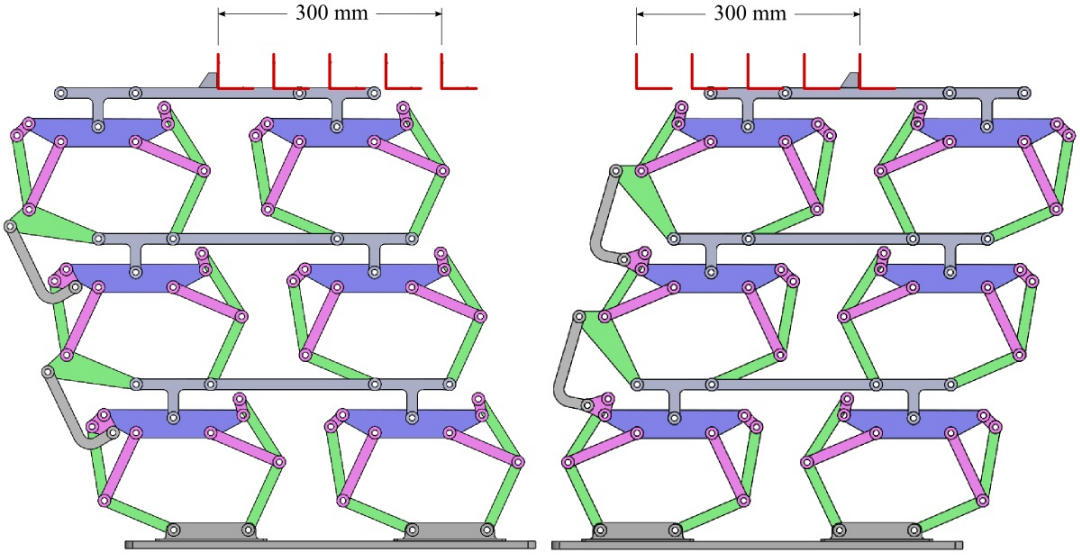

Figure 10: SolidWorks rendering of the selected eight-bar linkage from Example 1 stacked in three levels for amplifying the rectilinear movement from 100mm to 300mm.

Figure 9 is an example of a successful design, which in this case is formed by the RR dyads (24)(46). The coordinates of the 10 pivots, $(C_1, \ldots, C_{10})$, are listed in Table 4. This linkage deviates from the rectilinear task requirements by a maximum of 0.5 micro radians and 26.5 micrometers in the y-direction.

The structure of this eight-bar linkage has the property that it can be assembled in layers to amplify the rectilinear movement, Figure 10. The

Table 4: Selected eight-bar linkage solution for Example 1

Pivot	Location(x, y)
C_1	$(-50.00, -150.00)$
C_2	$(-142.11, -110.81)$
C_3	$(-100.00, -20.00)$
C_4	$(0.00, -20.00)$
C_5	$(91.98, -59.24)$
C_6	$(50.00, -150.00)$
C_7	$(-164.50, -13.25)$
C_8	$(-146.05, 3.48)$
C_9	$(46.10, 3.42)$
C_{10}	$(43.42, 28.18)$

layers are interconnected by a four-bar function generator so the system moves with one degree of freedom, and provides a maximum deviation in the y direction of 79.5 micrometers.

9.2. Offset Task Positions

For this design, each of the task positions in Table 1 are shifted in the x direction by the amount of 50mm. Thus, the 6R loop is centered on the first task position and the remaining are placed over the range of 100mm in the positive x direction. The coordinates of the 6R loop has the same dimensions as in the first example, but the new placement of the task positions yields a new set of coordinates, Table 5. As before random variations within $\pm$5mm were introduced to the coordinates of the base pivots C_1 and C_6 for each iteration. The results of the calculations are presented in Table 6.

An example eight-bar linkage obtained from this calculation is shown in Figure 11. The linkage is obtained by constraining the 6R closed chain robot with two RR constraints (26)(35). The coordinates of its 10 joints, $(C_1, \ldots, C_{10})$, are provided in Table 7. The maximum angular deviation from horizontal is 5 micro radians and the maximum vertical deviation from the straight line is 5.23 micrometers.

Table 5: 6R closed chain data for Example 2

Pivot	Location Data (x, y)
C_1	$(50.00, -150.00)$
C_2	$(-126.12, -85.00)$
C_3	$(-50.00, -20.00)$
C_4	$(50.00, -20.00)$
C_5	$(125.99, -85.00)$
C_6	$(50.00, -150.00)$

Table 6: Multi-iteration run for the design algorithm for Example 2

Iterations	Candidate Linkages	Successful Designs	Computation Time
1	60	5	1.74 min
10	741	65	15.61 min
100	7857	584	1 hr 52.80 min

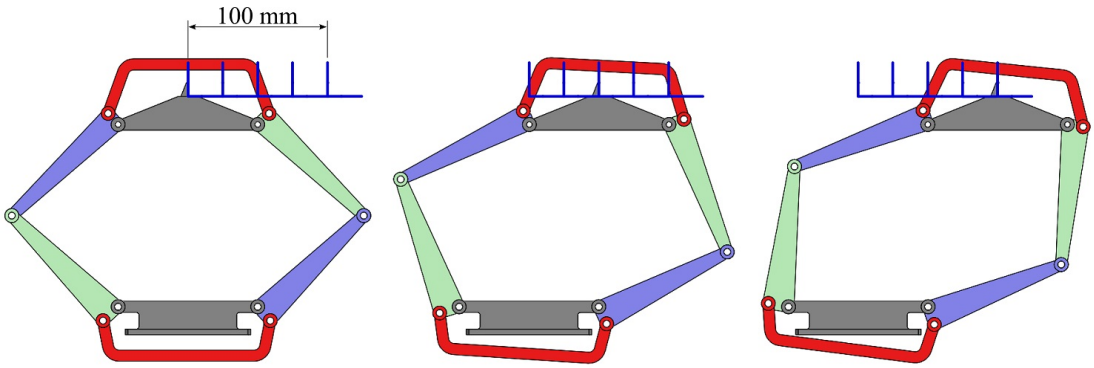

Figure 11: An eight-bar linkage design obtained for the offset set of task positions.

10. Conclusions

This paper presents a design system for eight-bar linkages that uses five-position synthesis to computer two RR dyads that constrain a planar 6R loop. A systematic procedure yields as many as 340 candidate designs that

Table 7: Selected eight-bar linkage solution for Example 2

Pivot	Location Data (x, y)
C_1	$(50.00, -150.00)$
C_2	$(-126.12, -85.00)$
C_3	$(-50.00, -20.00)$
C_4	$(50.00, -20.00)$
C_5	$(125.99, -85.00)$
C_6	$(50.00, -150.00)$
C_7	$(-60.80, -159.89)$
C_8	$(59.01, -159.91)$
C_9	$(-57.08, -12.10)$
C_{10}	$(58.18, -12.11)$

are evaluated to ensure they meet the task requirements. Random variations of the requirements within user-defined tolerance zones increase the number of successful eight-bar linkage designs.

This design system is demonstrated by calculating the dimensions of eight-bar linkages that guide an end-effector through five parallel task positions along a straight line. In one case the task positions are placed symmetrically relative to the 6R loop and the second they are offset to one side.

A single iteration of this algorithm required one and two minutes respectively, and yielded over 40 successful eight-bar linkages designs for both cases. 100 iterations required approximately 1 hour and 2 hours for the respective cases, and yielded thousands of successful designs. This system provides a practical methodology for the design of these complex mechanical systems.

11. Acknowledgements

This material is based upon work supported by the National Science Foundation under Grant No. CMMI 1066082.

References

Burmester, L., *Lehrbuch der Kinematik, Vol. 1, Die ebene Bewegung*, Leipzig, 1888.

Chen, C., and Angeles, J., "A novel family of linkages for advanced motion synthesis," *Mechanism and Machine Theory*, 43(7), 882-890, 2008.

Hain, K., "The Simultaneous Production of Two Rectilinear Translations by Means of Eight-link Mechanisms," *Journal of Mechanisms*, Vol. 2, No. 2, pp. 185-191, 1967.

Hamid, S., and Soni A. H., "Synthesis of an Eight-Link Mechanism for Varieties of Motion Programs," *Journal of Engineering for Industry*, 95, no. 3, pp. 744-750, 1973.

Kempe, A. B. , *How to Draw a Straight Line; A Lecture on Linkages*, McMillan and Co., London, 1877.

Koetsier, T., "The centenary of Ludwig Burmeister's Lehrbuch der Kinematik," *Mechanism and Machine Theory*, 1:37-38, 1989.

McCarthy, J. M., and Choe, J., "Difficulty of Kinematic Synthesis of Usable Constrained Planar 6R Robots," *Advances in Robot Kinematics*, 12th International Symposium, June 28 July 1, 2010, Portoroz, Slovenia.

McCarthy, J. M. and Soh, G. S., *Geometric Design of Linkages. 2nd Ed.*, Springer-Verlag, 2010.

Mueller, J., Dissertation: "Design Procedures for the Determination of Dimensions of Eight-bar and Ten-bar Linkages," 1954, Technische Universitat Dresden, Germany.

Murray, R. M., Li, Z., and Sastry, S. S., *A Mathematical Introduction to Robotics Manipulators*, CRC Press, 1994, 456 pp.

Parrish, B. E, McCarthy, J. M., and Eppstein, D., "Automated Generation of Linkage Loop Equations for Planar 1-DoF Linkages, Demonstrated up to 8-bar," *ASME Journal of Mechanisms and Robotics*, Vol. 6, December 2014.

Plecnik, M. M. and McCarthy, J. M., "Design of a 5-SS Spatial Steering Linkage," DETC 2012-71405, *Proceedings of the ASME 2012 International Design Engineering Technical Conferences and Computers and Information in Engineering Conferences*, August 12-15, 2012, Chicago, IL, USA.

Plecnik, M. M. and McCarthy, J. M., "Numerical Synthesis of Six-bar Linkages for Mechanical Computation," *Journal of Mechanisms and Robotics*, 2013.

Sandor, G. N., and Erdman, A. G., *Advanced Mechanism Design: Analysis and Synthesis, Vol. 2*. Prentice-Hall, Englewood Cliffs, NJ, 1984.

Soh, G. S., and McCarthy, J. M., "Synthesis of Eight-Bar Linkages as Mechanically Constrained Parallel Robots," *12th IFToMM world congress A*, Vol. 653, 2007.

Sonawale, K. H., Arredondo, A., and McCarthy, J. M., "Computer Aided Design of Useful Spherical Watt I Six-bar Linkages," *Proceedings of the ASME 2013 International Design Engineering Technical Conferences & Computers and Information in Engineering Conference*, DET2013-13454, August 4-7, 2013, Portland, Oregon USA.

Sonawale, K. H., Dissertation: *Computer Aided Design of Eight-Bar Linkages* University of California, Irvine, CA, USA, 2014.

Sonawale, K. H., and McCarthy, J. M., "Synthesis of Useful Eight-bar Linkages as Constrained 6R loops," *Proceedings of the ASME 2014 International Design Engineering Technical Conferences and Computers and Information in Engineering Conference*, DET2014-35523, August 17-20, 2014, Buffalo, New York, USA.

Sonawale, K. H., and McCarthy, J. M., "Design of Eight-bar Linkages for Rectilinear Motion," *Proceedings of the ASME 2015 International Design Engineering Technical Conferences and Computers & Information in Engineering Conference*, DETC 2015-47804, August 2-5, 2015, Boston, Massachusetts, USA.

Sonawale, K. H., and McCarthy, J. M., "A Design System for Eight-bar Linkages as Constrained 4R Serial Chains," under review *ASME Journal of Mechanisms and Robotics*, March 2015.

Tsai, L. W., *Mechanism Design: Enumeration of Kinematic Structures According to Function*, CRC Press, 2000.

DeGarmo, E. P., Black, J. T., and Kohser, R. A., "Materials and Processes in Manufacturing," John Wiley & Sons, 2011.

Appendix: Eight-bar linkage graphs obtained by attaching two RR constraint to a 6R closed chain

The 32 linkage graphs $(ij)(kl)$ are separated into (i) independent constraints that have $i, j, k, l \in \{1, 2, 3, 4, 5, 6\}$, Fig.12, and (ii) dependent constraints that have $i, j, k \in \{1, 2, 3, 4, 5, 6\}$ and $l \in \{7\}$, Fig.13.

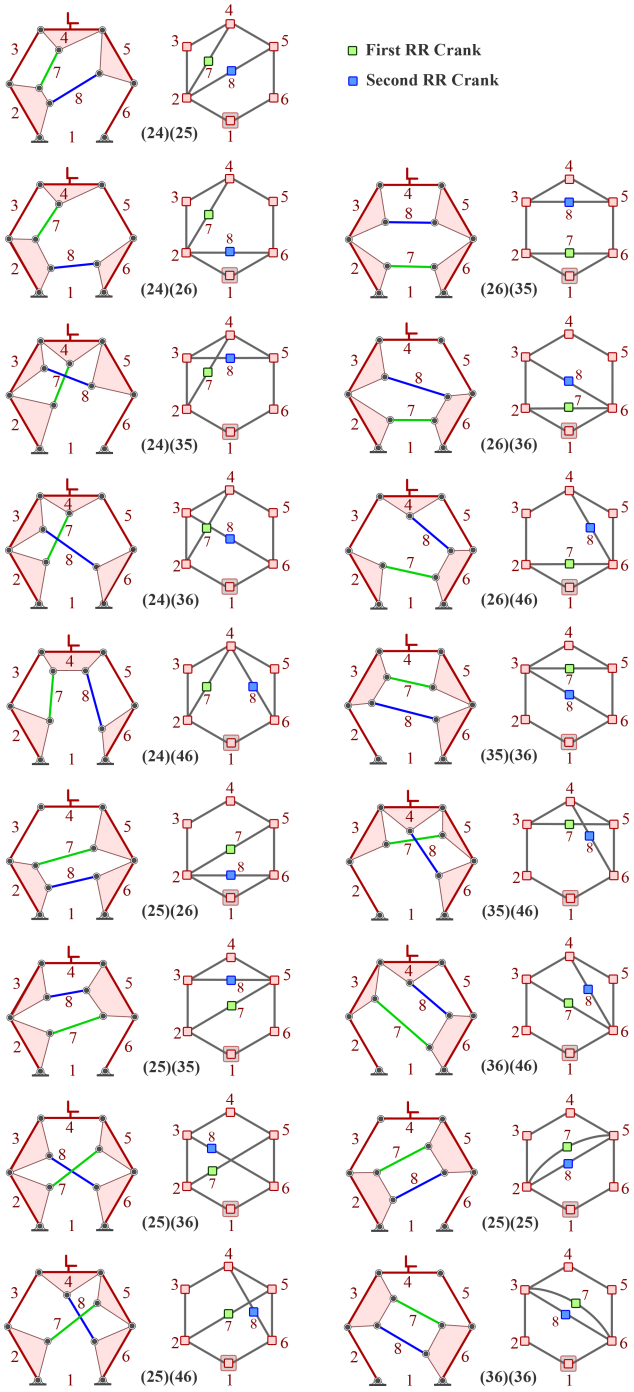

Figure .12: The 17 eight-bar linkage graphs $(ij)(kl)$ obtained by adding two independent RR dyads, with $i, j, k, l \in \{1, 2, 3, 4, 5, 6\}$.

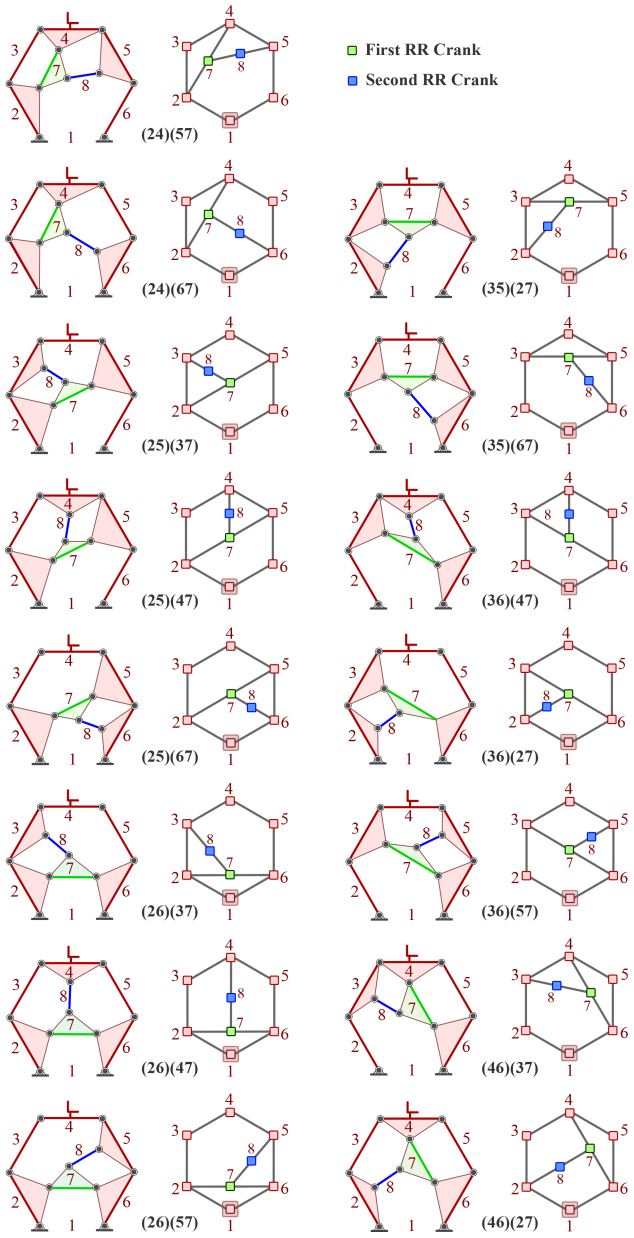

Figure .13: The 15 eight-bar linkage graphs $(ij)(kl)$ obtained by adding the second RR dyad to the link of the first RR dyad, that is with $i, j, k \in \{1, 2, 3, 4, 5, 6\}$ and $l \in \{7\}$.